

# Rectangular-Shaped Expanded Phthalocyanines with Two Central Metal Atoms

Osamu Matsushita,<sup>†</sup> Valentina M. Derkacheva,<sup>‡</sup> Atsuya Muranaka,<sup>§,||</sup> Soji Shimizu,<sup>†</sup> Masanobu Uchiyama,<sup>§,⊥</sup> Evgeny A. Luk'yanets,<sup>\*,‡</sup> and Nagao Kobayashi<sup>\*,†</sup>

<sup>†</sup>Department of Chemistry, Graduate School of Science, Tohoku University, Sendai 980-8578, Japan

<sup>‡</sup>Organic Intermediates and Dyes Institute, B. Sadovaya 1/4, Moscow 123995, Russia

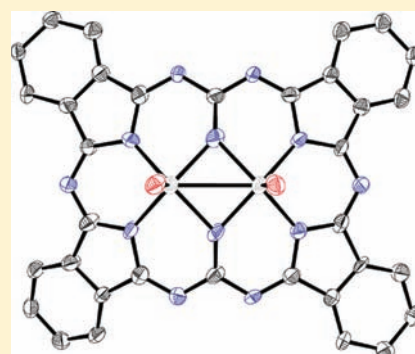
<sup>§</sup>Advanced Elements Chemistry Research Team, ASI, RIKEN, Wako 351-0198, Japan

<sup>||</sup>PRESTO, Japan Science and Technology Agency (JST), Saitama 332-0012, Japan

<sup>⊥</sup>Graduate School of Pharmaceutical Sciences, The University of Tokyo, Bunkyo-ku, Tokyo 113-0033, Japan

## Supporting Information

**ABSTRACT:** Expanded phthalocyanine (Pc) congeners with two Mo or W central metal ions and four isoindole ring moieties have been synthesized using normal Pc formation conditions in the presence of urea. The products have been characterized by electrochemistry; mass spectrometry (MS); IR, electron paramagnetic resonance (EPR), NMR, electronic absorption, and magnetic circular dichroism (MCD) spectroscopies; and X-ray analysis. The X-ray structures have rectangular  $C_{2v}$  symmetry and provide evidence that the central Mo atoms are linked by a single bond and coordinated by two isoindole nitrogen atoms and two nitrogen atoms from the amine moieties. The electronic absorption bands extend into the 1200–1500 nm region. This can be explained using Gouterman's four-orbital theory. The experimental NMR data and theoretical calculations provide evidence for a heteroaromatic 22- $\pi$ -electron conjugation system for the ring-expanded Pc system, which satisfies Hückel's  $(4n + 2)\pi$  aromaticity.



## INTRODUCTION

Ever since Linstead's initial report in 1934,<sup>1</sup> phthalocyanines (Pcs) have been used as industrial materials. In recent years, new applications in storage media, organic semiconductors, laser printers, photodynamic therapy of cancer, nonlinear optics, and deodorants due to the stability of the compounds and the intense absorption bands in the visible region have been reported.<sup>2,3</sup> Pcs can therefore be said to play a central role in modern society. In recent years, more than 2000 patents and research papers have been reported annually.<sup>4</sup>

A number of different synthetic methods have been reported for metallo-Pcs. Template reactions in the presence of a transition metal or metal salts are the most common. Systems containing a phthalic anhydride, phthalimide, phthalamide, or phthalonitrile in the presence of urea, or a 1*H*-isoindole-1,3(2*H*)-diimine are often used. In the presence of most metals, normal, planar Pcs consisting of four isoindole moieties and having approximate  $D_{4h}$  symmetry are obtained. In the presence of lanthanoids, double- and in rare cases even triple-decker sandwich-type Pc complexes are obtained.<sup>5</sup> When boron or uranium ions are reacted with a phthalonitrile, cone-shaped Pc analogues consisting of three isoindole rings [so-called subphthalocyanines (SubPcs)] or deformed Pc derivatives consisting of five isoindole rings [super-phthalocyanines (SuperPcs)] are formed (Figure 1) because of the smaller or larger ionic radii, respectively, relative to first-row transition

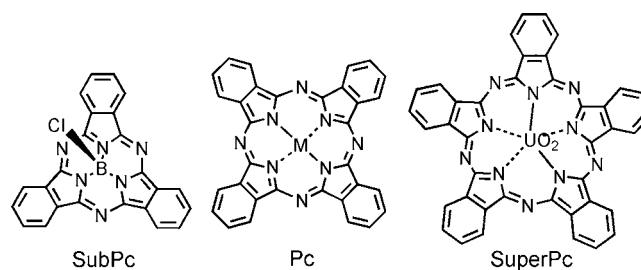


**Figure 1.** Structures of phthalocyanine derivatives.

metals.<sup>6,7</sup> Although more than 300 X-ray structures have been reported for metallo-Pcs,<sup>8</sup> SubPcs, and SuperPcs, all of these compounds contain isoindole rings connected by aza nitrogen atoms whether they are monomeric, dimeric, or oligomeric, and no other complex types have been reported from these Pc formation reactions.<sup>7,9</sup> In this article, we provide the first report of a completely new type of Pc complex containing two metal ions that is obtained under normal Pc formation reaction conditions in the presence of molybdenum and tungsten salts.

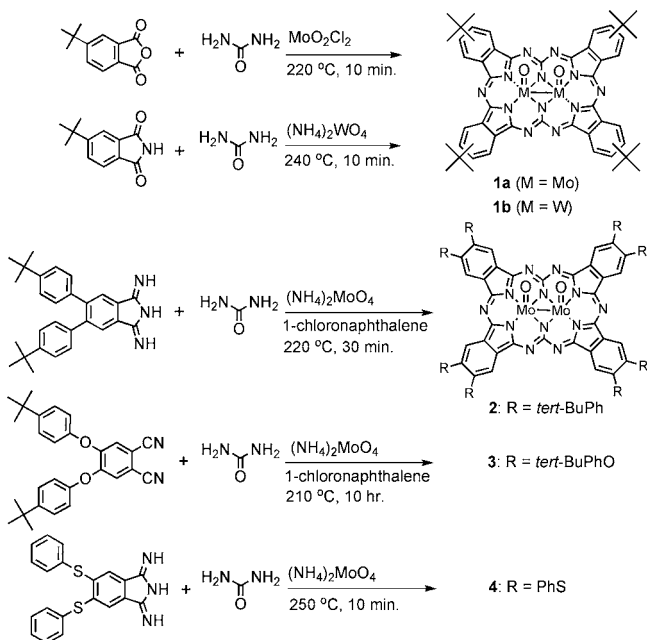
**Received:** October 12, 2011

**Published:** February 8, 2012

## RESULTS AND DISCUSSION

**Synthesis and MS Analysis.** In a similar manner to normal Pc formation reactions,<sup>9</sup> a mixture of phthalic anhydride or phthalimide and excess urea (and occasionally a trace amount of 1-chloronaphthalene for ease of stirring; see Scheme 1) was

Scheme 1. Syntheses of 1–4



heated in the presence of a molybdenum [ $\text{MoO}_2\text{Cl}_2$  or  $(\text{NH}_4)_2\text{MoO}_4$ ] or tungsten salt [ $(\text{NH}_4)_2\text{WO}_4$ ] at 210–250 °C for 10–30 min, and the products were purified by chromatography using silica gel followed by a size-exclusion column. After removal of greenish-blue bands containing normal Pcs, another band with a brown color was collected, and strong electronic absorption bands beyond 900 nm were detected. The yields were always higher for molybdenum salts (max. 8.3%) than for tungsten salts (less than 2.0%). The tungsten derivatives tended to decompose during column chromatography. Although the yield was low, a similar compound (**3**) was obtained even when phthalonitrile and urea were used as the starting materials. The absorption spectra of each of these compounds did not change upon storage for up to a year so long as they were kept in the dark in the solid state. This demonstrates that these compounds are reasonably stable. However, when the complexes were dissolved in solution or stored under direct light, they decomposed more slowly than ZnPc but more quickly than CuPc.

All of the brown compounds with intense absorption bands beyond 900 nm were subjected to analysis by mass spectrometry (MS). As shown in Figure S1 in the Supporting Information (SI), the high-resolution MS (HR-MS) spectra and calculated isotopic distribution patterns provided a reasonable match for the compounds with two atoms of molybdenum (**1a**, **2**, and **3**) or tungsten (**1b**). To provide a further confirmation of the number of nitrogen atoms,  $^{15}\text{N}$ -labeled **1a** was synthesized using  $^{15}\text{N}$ -labeled urea. The parent peak was observed by HR-MS at  $m/z$  1076.1677 [ $\text{M}^+ + \text{Na}$ ], while  $m/z$  1076.1678 was calculated for  $\text{C}_{50}\text{H}_{48}\text{Mo}_2^{15}\text{N}_{12}\text{O}_2\text{Na}$ . The theoretical isotopic distribution pattern matched the experimental one almost perfectly (Figure S1 in the SI). When the

mass data obtained for **4** were also taken into consideration, all of the mass data could be successfully reproduced only when 12 nitrogen atoms, two oxygen atoms, and two molybdenum or tungsten atoms were included.

**X-ray Crystal Analysis.** Crystallization was attempted for **2–4**, and fortuitously, single crystals suitable for X-ray diffraction analysis were obtained by slow diffusion of ethanol into a solution of **2** in 1-chloronaphthalene. The crystal structure of **2** (Figure 2)<sup>10</sup> reveals that the macrocycle

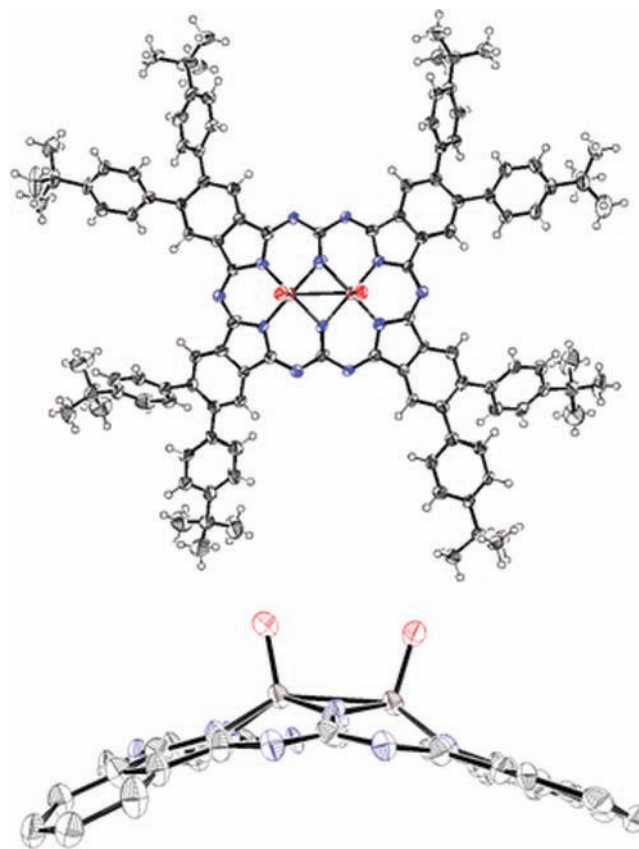


**Figure 2.** X-ray crystal structure of **2**: (top) top view; (bottom) side view. The thermal ellipsoids are scaled to the 50% probability level. For clarity, H atoms and substituents have been omitted in the side view.

comprises four isoindole rings linked by two methanetriamine moieties and contains two Mo ions in its central cavity. Two oxygen atoms are connected to each Mo ion from the same direction as axial ligands (i.e., a *cis* isomer).<sup>11</sup> The Mo–O bonding distance of 1.66 Å in the crystal structure is in the range of lengths for Mo=O double bonds.<sup>12,13</sup> The interatomic distance between the two Mo ions is 2.64 Å, which corresponds to the distance of a Mo–Mo single bond.<sup>14</sup> Each Mo ion is further coordinated by two pyrrole nitrogen atoms and two amino nitrogen atoms of the macrocycle (**5A** in Figure 3). The overall molecular structure of **2** adopts a dome shape. The dihedral angles formed by the isoindole moieties are 39° on average. The Mo ions lie out of the macrocyclic plane. No significant bond-length alternation was observed for the C–N and C–C bonds of the core structure of **2** (Figure S2 in the SI), as would be anticipated for a heteroatomic  $\pi$  system. This pattern is generally observed in the crystal structures of Pc congeners. On the basis of the MS and  $^1\text{H}$  NMR data described below, the only other isomer that could be formed would

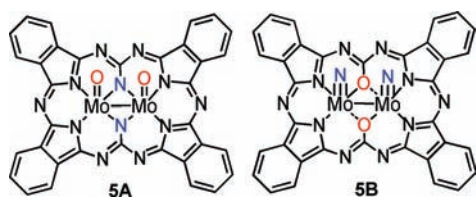


**Figure 3.** Possible structures **5A** and **5B** based on the MS and  $^1\text{H}$  NMR analyses.

contain two nitride-type nitrogen atoms connected at the axial positions and two oxygen atoms in turn residing at the meso positions to coordinate each Mo ion along with two pyrrole nitrogen atoms in a square planar fashion (**5B** in Figure 3). A detailed analysis of both structures revealed that the thermal ellipsoids were properly solved for the structure **5A** in Figure 3.

**$^1\text{H}$  NMR Spectra.**  $^1\text{H}$  NMR signals of **1–4** appeared in the same region as those observed for conventional Pc congeners,<sup>7</sup> providing strong evidence that the compounds are diamagnetic.

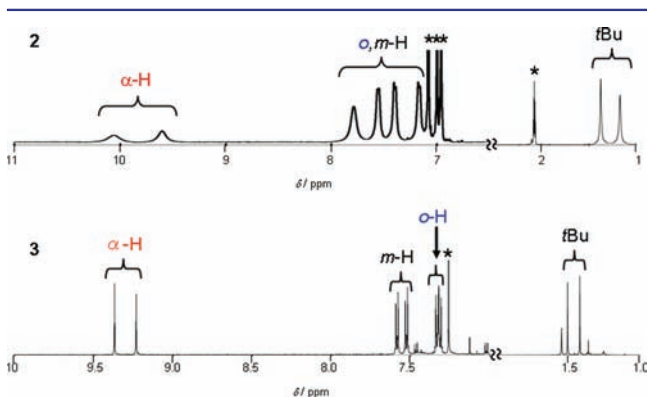


**Figure 4.**  $^1\text{H}$  NMR spectra of **2** in toluene- $d_8$  (top) and **3** in  $\text{CDCl}_3$  (bottom). \* indicates residual solvent peaks.

Figure 4 contains the spectra of **2** and **3**, and the details of the  $^1\text{H}$  NMR data for all of the compounds are described in the Experimental Section. The signals of **3** were assigned on the basis of both correlation spectroscopy (COSY) and nuclear Overhauser effect (NOE) experiments (Figures S3 and S4 in the SI). Two  $\alpha$ -benzo proton signals appear at 9.23 and 9.37 ppm as singlets with the same intensity, while *tert*-butyl proton signals were found at 1.42 and 1.51 ppm, indicating that **3** possesses a symmetry lower than the regular  $D_{4h}$  symmetry of metallo-Pcs. On the other hand, the four doublets of the phenoxy protons observed in the 7.3–7.6 ppm region are similar to those at 7.1–7.3 ppm for 2,3,9,10,16,17,23,24-octa(*p-tert*-butyl)phenoxy zinc phthalocyanine (*t*-BuPhOZnPc). The fact that signals due to the  $\alpha$ -benzo protons of **3** appeared significantly downfield relative to the corresponding protons of 4,5-di-*tert*-butylphenoxyphthalonitrile (7.82 ppm in  $\text{CDCl}_3$ )<sup>15</sup> is consistent with the presence of a strong ring-current effect and a heteroaromatic  $\pi$  system. Similar trends as shown for **2** and **3** (Figure 4) have been proposed for the  $^1\text{H}$  NMR spectra of **1** and **4**.

**IR and EPR Spectra.** When a Mo salt is used as a template in Pc syntheses in the presence of urea, nitride complexes of MoPc [(Mo<sup>V</sup>≡N)Pc] are known to be formed.<sup>16</sup> For the (Mo<sup>V</sup>≡N)Pcs reported to date, the IR signals associated with the Mo<sup>V</sup>≡N bond are observed in the 950–980  $\text{cm}^{-1}$  range,

while an intense electron paramagnetic resonance (EPR) signal due to the coupling of the unpaired electron with the five nitrogen atoms is observed at  $g \approx 1.97$ , along with weaker lines on each side due to electron–Mo<sup>95</sup>/Mo<sup>97</sup> coupling.<sup>17</sup> In this study, during the purification of **1a**, tetra-*tert*-butylated (Mo<sup>V</sup>≡N)Pc was obtained (HR-MS:  $m/z$  871.2985 found for [M<sup>+</sup> + Na];  $m/z$  871.2984 calcd for  $\text{C}_{48}\text{H}_{48}\text{MoN}_9\text{Na}$ ), and the anticipated IR band was observed at 974  $\text{cm}^{-1}$ , while an EPR signal was detected at  $g = 1.977$  in toluene at room temperature (Figure S6 in the SI). When the IR spectrum of **1a** obtained from the same batch as the *tert*-butylated (Mo<sup>V</sup>≡N)Pc was recorded, the spectrum shown in Figure 5 was obtained. **1a** was

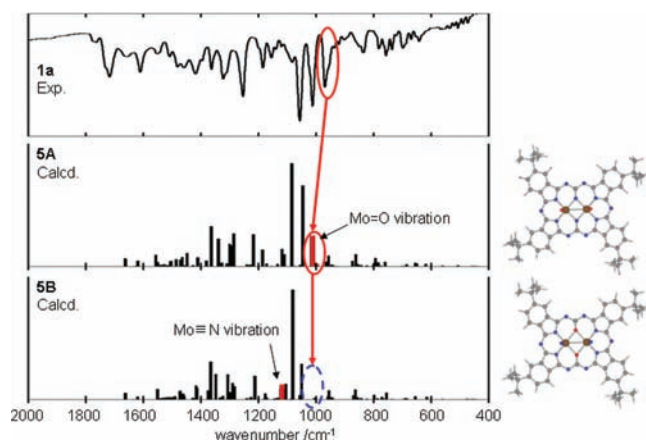


**Figure 5.** Observed IR spectrum of **1a** (top) and theoretical IR spectra of structures **5A** (middle) and **5B** (bottom) with *tert*-butyl substituents. Red bars indicate the vibrations involving Mo and its axial ligand.

found to be EPR-silent under the same conditions, which is reasonable considering the coordination geometry around the Mo ions and the presence of a Mo–Mo single bond as observed in the crystal structure of **2** (Figure 2). Since the IR spectra of high-symmetry ( $D_{4h}$ ) and low-symmetry Pc derivatives can be reliably reproduced by theoretical calculations in terms of both the energies and intensities of bands,<sup>18</sup> calculated IR spectra were obtained for structures **5A** and **5B** (Figure 3) and compared with the experimental data for compound **1a** (Figure 5). A structure substituted with *tert*-butyl groups was optimized. Although the calculated spectra for **5A** and **5B** broadly reproduced the experimental data, we focused our attention on the 1080–970  $\text{cm}^{-1}$  region since **1a** displays three intense characteristic peaks at 1057, 1012, and 970  $\text{cm}^{-1}$ . As is clearly shown in Figure 5, these three strong peaks were reproduced when the Mo<sup>V</sup>=O structure (**5A**) was used, while in contrast, when the Mo<sup>V</sup>≡N structure (**5B**) was used only two intense peaks were predicted. Of the three intense peaks calculated for structure **5A**, the peak at the lowest energy (1014  $\text{cm}^{-1}$ ) corresponds to the peak observed at 970  $\text{cm}^{-1}$ , which can be assigned as a Mo<sup>V</sup>=O stretching vibrational mode. The Mo<sup>V</sup>=O stretching vibrational modes of Pcs that have been reported previously have always appeared in the 970–975  $\text{cm}^{-1}$  region,<sup>19</sup> while that of Mo<sup>V</sup>≡N has been reported to lie between 950–980  $\text{cm}^{-1}$ .<sup>17</sup> These results therefore suggest that the compounds formed have a Mo<sup>V</sup>=O structure (**5A**).<sup>20</sup>

**Absorption, MCD, and Fluorescence Spectra.** The absorption, magnetic circular dichroism (MCD), and fluorescence spectra of **2** are shown in Figure 6, together with the absorption and MCD spectra of *tert*-butylated  $\text{H}_2\text{Pc}$  (*t*-

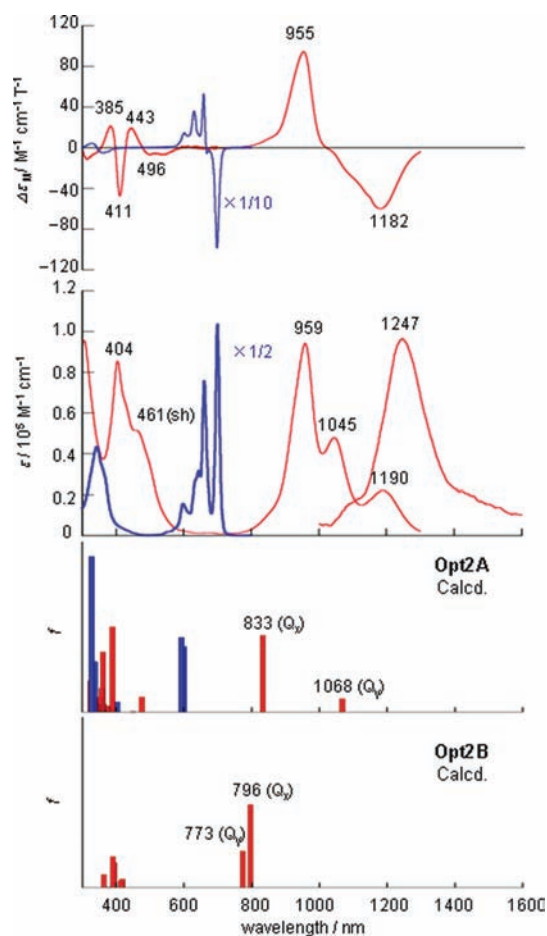


**Figure 6.** Absorption (middle) and MCD (top) spectra of **2** (red) and *t*BuH<sub>2</sub>Pc (blue) in CHCl<sub>3</sub> and theoretical absorption spectra (bottom) of **Opt2A** and **Opt2B** (red) and H<sub>2</sub>Pc (blue). The fluorescence spectrum of **2** in CHCl<sub>3</sub> is also shown in the middle panel.

BuH<sub>2</sub>Pc); the absorption and MCD spectra of **1**, **3**, and **4** can be compared in Figure 7. The spectra of **1–4** are broadly similar and contain bands that can be readily assigned as the Q and B bands in the context of Gouterman's four-orbitals terminology<sup>21</sup> (strictly speaking, the Q band is probably better described as the L band in Platt's terminology,<sup>22</sup> since the angular momentum change ( $\Delta M_L$ ) of the Q band is  $\pm 9$  while for **1–4** it is  $\pm 11$ ). The peak at longest wavelength is substantially red-shifted into the near-IR region relative to that of *t*-BuH<sub>2</sub>Pc, reflecting the expansion of the aromatic  $\pi$  systems of **1–4** relative to those of conventional Pcs. The MCD spectra in the Q-band region are clearly dominated by Faraday B terms,<sup>23–25</sup> since the intensity maxima and minima are closely aligned with the centers of the main absorption bands. This provides direct spectral evidence that the molecular symmetry of the compounds is lower than C<sub>3</sub> and that the excited states are nondegenerate, as would be anticipated on the basis of the C<sub>2v</sub> symmetry of the crystal structure of **2**. The MCD bands observed in the 1000–1300 nm and 800–1000 nm regions can be assigned to symmetry-split  $y$ - and  $x$ -polarized Q<sub>00</sub> bands, since coupled oppositely signed B terms would be anticipated in this context. Although three peaks are generally observed in the absorption spectra in Figures 6 and 7, the second-lowest-energy band appears to be a vibrational component of the lowest-energy band, since the MCD signs are the same and the splittings between these bands are 1000–1200 cm<sup>-1</sup>, which is

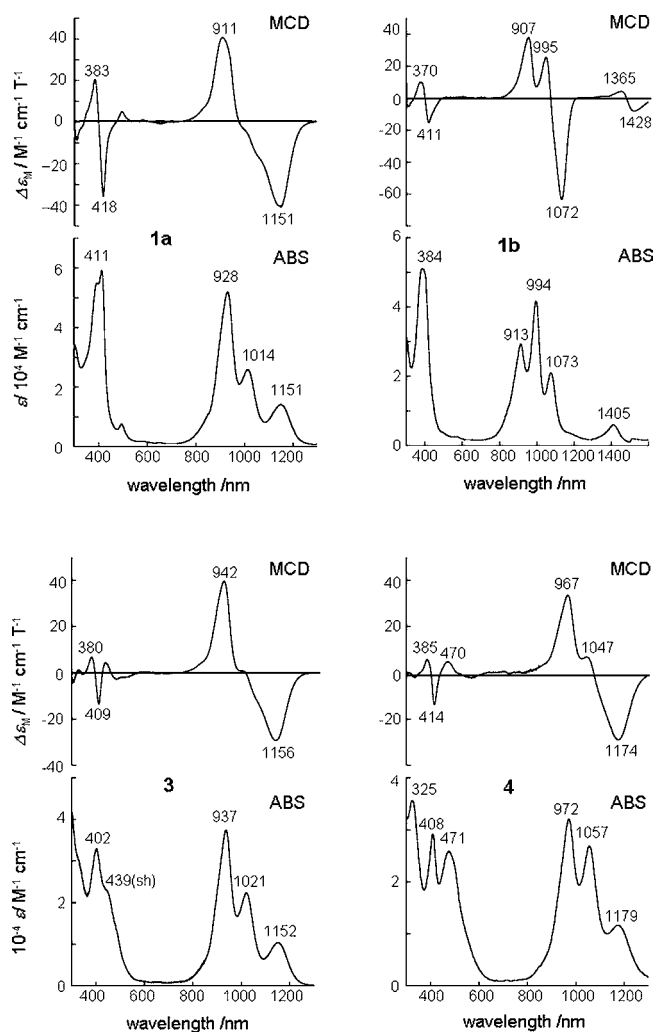


**Figure 7.** Absorption (bottom) and MCD (top) spectra of **1a**, **1b**, **3**, and **4** in CCl<sub>4</sub>.

typical of the spacing observed for vibrational bands in Pc spectra (ca. 1100 cm<sup>-1</sup>).<sup>23,26</sup> The optical spectra therefore provide strong evidence that compounds **1–4** arise from ring-expanded Pc analogues, which lack fourfold-symmetry axes.

The calculated absorption spectra based on structures containing Mo<sup>V</sup>=O (**5A**) and Mo<sup>V</sup>≡N (**5B**) are provided in the bottom portion of Figure 6 (for details, see the next section). The closest match with the experimental spectrum was obtained using the Mo<sup>V</sup> ion with an oxygen atom as the axial ligand.

Compound **2** was found to have a weak emission peak at 1247 nm when excited at 404 nm (Figure 6 middle).

**Analysis of  $\pi$ -Electron Structure.** Theoretical calculations were carried out using the Gaussian 03 software package<sup>27</sup> to provide further insight into the electronic structures. Geometry optimization calculations were carried out using the structure of **5A** as a model compound. The optimized structure, **Opt2A** (Figure S7 in the SI), is very similar to the crystal structure of **2**. In addition, the theoretical absorption spectrum (Figure 6) and a molecular orbital (MO) diagram (Figure 8) were calculated for **Opt2A** using time-dependent density functional theory (TD-DFT) (B3LYP/6-31G(d) for C, H, N, and O and LANL2DZ for Mo)<sup>28</sup> and compared with those of substituent-free H<sub>2</sub>Pc. The symmetry-split Q bands of **Opt2A** were

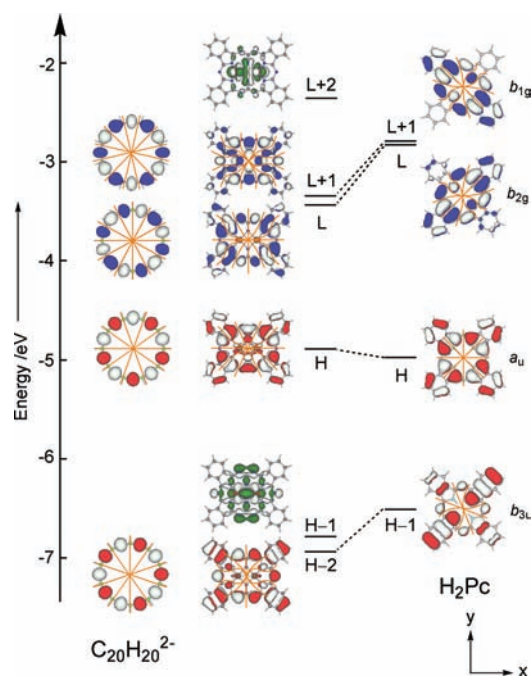


**Figure 8.** MO diagrams of **Opt2A** and **H<sub>2</sub>Pc**. H and L indicate the HOMO and LUMO, respectively. Arbitrary nodal lines have been drawn on the isosurface plots.

predicted to lie at 1068 and 833 nm, while those of **H<sub>2</sub>Pc** were predicted to lie at 601 and 594 nm. The large splitting of the two bands ( $2642\text{ cm}^{-1}$ ) and the much weaker intensity of the lower energy band of **Opt2A** ( $f = 0.080$  compared with  $f = 0.45$ ) are in close agreement with the experimental data (splitting =  $2025\text{ cm}^{-1}$  and intensity ratio  $\approx 1:5$ ; Figure 6). The Q bands were predicted to arise primarily from the four frontier  $\pi$ -MOs (Table 1). The HOMO–1 was not included since it is derived mainly from d orbitals of the two Mo atoms. When **Opt2B**, which is based on the structure of **5B** with an  $\text{Mo}^{\text{V}}\equiv\text{N}$  core structure, was used instead, the Q bands were calculated to lie at 796 and 773 nm with a splitting of only  $374\text{ cm}^{-1}$ , and the intensity ratio was the opposite of that observed experimentally. This provides further evidence that an  $\text{Mo}^{\text{V}}\equiv\text{N}$  core structure is unlikely to be present.

In Figure 8, the HOMO–LUMO gap of **Opt2A** is much smaller than that of **H<sub>2</sub>Pc**. The marked red shift of the Q band of **2** relative to that of *t*-Bu $\text{H}_2\text{Pc}$  is readily explained on this

basis. The splitting of the LUMO and LUMO+1 is smaller than that of the HOMO and HOMO–2, as would be anticipated on the basis of the  $-/+$  sign sequence observed for the Q bands in the MCD spectrum in ascending energy terms. Michl has demonstrated that a  $-/+$  sign sequence is consistent with the orbital angular momentum properties that arise when the energy difference between the MOs derived from the HOMO of a parent hydrocarbon corresponding to the inner perimeter of the ligand (in this case the HOMO and HOMO–2) is larger than that between the MOs derived from the LUMO (in this case the LUMO and LUMO+1).<sup>29,30</sup> The number of nodes on the inner ligand perimeter of **Opt2A** frontier  $\pi$ -MOs is the same as the number observed for the frontier  $\pi$ -MOs of the  $\text{C}_{20}\text{H}_{20}^{2-}$  parent hydrocarbon perimeter. For example, five nodes are observed for the HOMO and HOMO–2 of **Opt2A** and the HOMO and HOMO–1 of  $\text{C}_{20}\text{H}_{20}^{2-}$ . On this basis, it can be stated that the four frontier  $\pi$ -MOs of **Opt2A** are similar to those of a 20-atom, 22- $\pi$ -electron annulene, which satisfies Hückel's  $(4n + 2)\pi$  aromaticity rule. The strong intensity of the Q band in the MCD spectrum relative to that observed for the B-band region is related to the  $\Delta M_L = \pm 11$  change in orbital angular momentum properties that would be anticipated for the Q bands of **1–4** if the  $\pi$  systems were heteroaromatic.<sup>21</sup> The TD-DFT results therefore provide strong support for the conclusion that **Opt2A** and therefore **1–4** have a heteroaromatic 22- $\pi$ -electron system.

**Electrochemistry.** Cyclic voltammograms of **1a** and *t*-Bu $\text{H}_2\text{Pc}$  were measured under similar conditions (Figure 9),

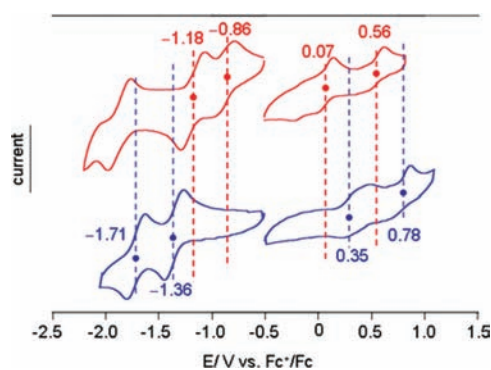


**Figure 9.** Cyclic voltammograms of **1a** (red lines) and *t*Bu $\text{H}_2\text{Pc}$  (blue lines). Conditions: sample, 1.0 mM; solvent, distilled *o*-DCB; electrolyte, 0.1 M TBAP; reference electrode, Ag/AgCl; counter electrode, Pt wire; scan rate, 100 mV/s.

**Table 1.** Transition Weights of Q Bands in **Opt2A**, **Opt2B**, and **H<sub>2</sub>Pc** Obtained Using the TDDFT Hamiltonian

	state	$\lambda$ (nm)	$f$	transition weight (density) <sup>a</sup>
<b>Opt2A</b>	$Q_y$	1068	0.080	H $\rightarrow$ L+1 (0.70)
	$Q_x$	833	0.45	H $\rightarrow$ L (0.70), H–2 $\rightarrow$ L+1 (0.14)
<b>Opt2B</b>	$Q_x$	796	0.49	H $\rightarrow$ L (0.57), H–2 $\rightarrow$ L (0.20)
	$Q_y$	773	0.22	H $\rightarrow$ L+1 (0.61), H–2 $\rightarrow$ L+1 (0.19)
<b>H<sub>2</sub>Pc</b>	$Q_x$	601	0.39	H $\rightarrow$ L+1 (0.60), H–1 $\rightarrow$ L (0.17)
	$Q_y$	594	0.44	H $\rightarrow$ L (0.60)

<sup>a</sup>H = HOMO; L = LUMO.

and four redox couples were observed for each [ $-1.18$ ,  $-0.86$ ,  $0.07$ , and  $0.56$  V vs  $\text{Fc}/\text{Fc}^+$  for **1a** and  $-1.71$ ,  $-1.36$ ,  $0.35$ , and  $0.78$  V for  $t\text{-BuH}_2\text{Pc}$ ]. The HOMO–LUMO energy difference for **1a** estimated on the basis of the potential difference between the first oxidation and first reduction ( $0.93$  V) is smaller than that of  $t\text{-BuH}_2\text{Pc}$  ( $1.71$  V), as would be anticipated from the red shift of the Q band of **1a** relative to  $t\text{-BuH}_2\text{Pc}$ . The potential difference of  $0.50$  V between the first reduction step of  $t\text{-BuH}_2\text{Pc}$  ( $-1.36$  V) and **1a** ( $-0.86$  V) was larger than the difference of  $0.28$  V between the first oxidation steps of these compounds ( $0.35$  and  $0.07$  V, respectively) (Figure 9). This is consistent with the prediction that the stabilization of the LUMO of **1a** relative to the normal Pc structure is larger rather than the destabilization of the HOMO (Figure 8). This is an important property of Pc derivatives, since the instability toward air of larger Pc congeners such as naphthalocyanine and anthracocyanine is consistently related to the destabilization of the HOMO.<sup>18a,26a</sup>

**NICS(0) Calculation.** Since the core structure was elucidated on the basis of the X-ray analysis of **2**, the aromaticity of this  $\pi$  system was evaluated by calculating nucleus-independent chemical shift (NICS) values.  $^1\text{H}$  NMR chemical shifts were calculated for the corresponding non-substituted metal-free structures using DFT with the B3LYP functional and 6-31G(d) basis sets.<sup>31</sup> The NICS values for expanded  $C_{2h}$ -symmetric Pcs (i.e., the metal-free  $\pi$  structures of **1–4**) were calculated to be  $-11.8$  ppm at the center of the structure and  $-11.3$  ppm at the center of the two central amino nitrogen and two pyrrole nitrogen atoms (i.e., the location of the Mo and W atoms in **1–4**), while a value of  $-13.5$  ppm at the center of  $D_{2h}$ -symmetric nonsubstituted metal-free  $\text{H}_2\text{Pc}$  was predicted (Figure 10). These values suggest that the expanded Pc has a ring-current effect similar to that of  $\text{H}_2\text{Pc}$ .

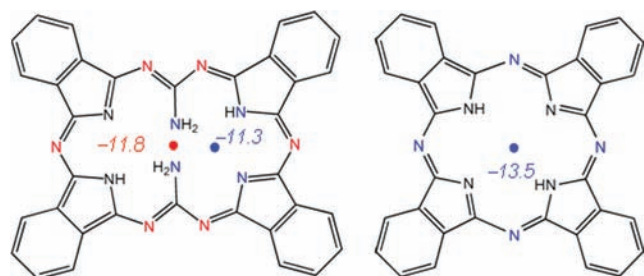


**Figure 10.** NICS values of the expanded  $C_{2h}$ -symmetric Pc analogue and  $D_{2h}$ -symmetric free-base Pc. NICS values for the expanded Pc at the centers of the inner 20-membered ring and the central heteroatoms are shown in red and blue, respectively.

## CONCLUSIONS

In summary, novel expanded phthalocyanine (Pc) congeners containing two  $\text{Mo}=\text{O}$  or  $\text{W}=\text{O}$  central cores and four isoindole moieties coordinated by four pyrrole nitrogen atoms and two amino nitrogen atoms have been synthesized under normal Pc formation conditions in the presence of urea. Their structures have been characterized using several spectroscopic methods, and their redox properties have been explored. X-ray analysis revealed a rectangular structure with  $C_{2v}$  symmetry. Although structures containing two  $\text{Mo}\equiv\text{N}$  or  $\text{W}\equiv\text{N}$  cores are also possible on the basis of the MS and  $^1\text{H}$  NMR data, careful analysis of the X-ray, IR, and electronic absorption data

and MO calculations has provided strong evidence for structures containing two  $\text{Mo}=\text{O}$  or  $\text{W}=\text{O}$  central cores. Electronic absorption bands in the  $1200\text{--}1500$  nm region were observed and could be readily assigned on the basis of Gouterman's four-orbital theory. Theoretical calculations were consistent with a heteroaromatic  $22\text{-}\pi$ -electron system, which satisfies Hückel's  $(4n + 2)\pi$  rule. Expanded Pc derivatives with absorption and emission bands in the NIR region have potential applications in fields such as solar cells and electroluminescence.

## EXPERIMENTAL SECTION

**General Procedures.** NMR spectra were recorded on 600 MHz JEOL ECA-600, 400 MHz Bruker AVANCE 400, and 400 MHz JEOL GSX-400 spectrometers. EPR spectra were measured in deaerated toluene at room temperature with a JEOL JES-FE2X spectrometer. IR spectra were measured by the KBr pellet method with a JASCO FT/IR 4100 spectrometer. High-resolution electrospray ionization Fourier transform ion cyclotron resonance (ESI-FT-ICR) mass spectra were recorded on a Bruker DALTONICS APEX III instrument. Electronic absorption spectra were measured using Hitachi U-3410 and JASCO V-570 spectrophotometers. MCD spectra in the  $300\text{--}700$  nm region were recorded using a JASCO J-725 spectrodichromometer with a JASCO electromagnet producing a magnetic field of up to  $1.09$  T, while spectra in the  $700\text{--}1300$  nm region were recorded using a JASCO J-730 spectrodichromometer with a JASCO electromagnet producing a magnetic field of up to  $1.50$  T. The magnitude of the MCD signal is expressed in units of magnetomolar circular dichroic absorption  $\Delta\epsilon_M$  ( $\text{M}^{-1}\text{cm}^{-1}\text{T}^{-1}$ ). Emission spectra were collected on a JASCO FP-6600 spectrofluorometer equipped with a Hamamatsu C9940 photomultiplier tube, using the surface photometric method.<sup>32</sup>

**Crystallographic Data Collection and Structure Refinement.** Data collection for **2** was carried out at  $-173$  °C on a Bruker APEXII CCD diffractometer with  $\text{Mo K}\alpha$  radiation ( $\lambda = 0.71073$  Å). The structure was solved by a direct method (SHELXS-97)<sup>33</sup> and refined using a full-matrix least-squares technique (SHELXL-97).<sup>33</sup> CCDC-830031 contains the supplementary crystallographic data. These data can be obtained free of charge from the Cambridge Crystallographic Data Centre via [www.ccdc.cam.ac.uk/data\\_request/cif](http://www.ccdc.cam.ac.uk/data_request/cif).

**Electrochemistry.** Cyclic voltammetry measurements were performed using a Hokuto Denko HZ5000 potentiostat under a nitrogen atmosphere in *o*-dichlorobenzene (*o*-DCB) solutions with  $0.1$  M tetrabutylammonium perchlorate (TBAP) as a supporting electrolyte. Measurements were made with a glassy-carbon electrode (area =  $0.07$   $\text{cm}^2$ ), a Ag/AgCl reference electrode, and a Pt wire counter electrode. The concentration of the solution was fixed at  $1.0$  mM, and the scan rate was  $100$  mV/s. The ferrocenium/ferrocene ( $\text{Fc}^+/\text{Fc}$ ) couple was used as an internal standard.

**Computational Methods.** DFT and TD-DFT calculations were performed using the Gaussian 03 software package using 6-31G(d) basis sets for C, H, N, and O and the LANL2DZ basis set for Mo. Optimized structures were obtained without symmetrization. Phthalocyanine ( $\text{H}_2\text{Pc}$ ) was optimized using  $D_{2h}$  symmetrization.

**Materials.** All commercial chemicals were used as received. 4-*tert*-Butylphthalic anhydride,<sup>34</sup> 4-*tert*-butylphthalimide,<sup>34</sup> and 4,5-bis(4-*tert*-butylphenoxy)phthalonitrile<sup>15</sup> were prepared according to methods described in the literature. The synthesis of 4,5-dibromophthalimide was carried out in high yield according to a published method<sup>35</sup> through initial oxidation of 4,5-dibromo-*o*-xylene<sup>36</sup> with  $\text{KMnO}_4$  in boiling 70% aqueous pyridine to form 4,5-dibromophthalic acid, followed by heating with ammonium acetate in acetic acid to form the target structure (mp:  $238\text{--}240$  °C).

**4,5-Di(phenylthio)phthalimide.** This compound was formed from by adding triethylamine ( $0.47$  g,  $4.6$  mmol) dropwise to a mixture of 4,5-dibromophthalimide ( $0.61$  g,  $2.0$  mmol) and thiophenol ( $0.51$  g,  $4.6$  mmol) in  $5$  mL of *N,N*-dimethylformamide. The stirred reaction mixture was kept at room temperature for  $1$  h and then at  $50\text{--}55$  °C for  $40$  min. After the mixture was cooled and poured into water, the

precipitate was filtered off, washed with water, and crystallized from acetic acid. Yellow crystals were obtained (yield: 0.50 g, 78%). Anal. (Calcd, Found for  $C_{20}H_{13}NO_2S_2$ ): C (66.09, 65.78), H (3.60, 3.45), N (3.85, 3.82), S (17.64, 17.61). Mp: 258–260 °C.

**1a.** A stirred mixture of 4-*tert*-butylphthalic anhydride (0.41 g, 2.0 mmol), urea (0.6 g, 10.0 mmol), and molybdenum(VI) dichloride dioxide (0.10 g, 0.5 mmol) was slowly heated for 50–60 min from 140 to 220 °C, and the temperature was then held for a further 10 min. The mixture of products was then cooled, extracted with  $CHCl_3$ , and passed through a silica gel column. The solvent was evaporated, and the residue was purified by column chromatography on silica gel using benzene as an eluent. The second colored fraction was collected after an initial fraction containing a trace amount of *t*-BuH<sub>2</sub>Pc had eluted. Further purification was achieved by gel-permeation chromatography on a Bio-Beads S-X1 column using  $CHCl_3$  as an eluent. After evaporation of the solvent, the residue was recrystallized from benzene and hexane to provide **1a** as a brown solid with a slight green tint (yield: 0.012 g, 4.6%). Anal. (Calcd, Found for  $C_{50}H_{48}Mo_2N_{12}O_2$ ): C (57.69, 56.75), H (4.65, 4.95), N (16.15, 15.58). HR-MS ( $m/z$ ): [ $M^+$  + Na] calcd for  $C_{50}H_{48}Mo_2N_{12}O_2Na$ , 1064.2033; found, 1064.2033.  $^1H$  NMR (600 MHz,  $CDCl_3$ ):  $\delta$  10.04, 9.90, 9.77, 9.71, 9.68, 9.66 (m, 8H), 8.55 (d,  $J$  = 7.9 Hz, 4H), 1.86 (m, 36H). UV/vis/NIR ( $CCl_4$ )  $\lambda_{max}/nm$  ( $\epsilon/M^{-1} cm^{-1}$ ): 1151 (14000), 1014 (26000), 928 (52000), 411 (59000). IR (KBr)  $cm^{-1}$ : 2957, 1717, 1655, 1611, 1551, 1508, 1482, 1458, 1419, 1396, 1364, 1324, 1254, 1185, 1155, 1141, 1120, 1083, 1057, 1012, 970, 936, 850, 836, 782, 758, 737, 699.

**1b.** A stirred mixture of 4-*tert*-butylphthalimide (1.02 g, 5.0 mmol), urea (3.0 g, 50.0 mmol), and ammonium tungstate (0.28 g, 1.0 mmol) was slowly heated for 60–70 min from 140 to 240 °C, and then the temperature was maintained for 10 min. The mixture was then cooled and extracted with chloroform, and insoluble impurities were removed by filtration. The crude product was purified on a silica gel column using a 2:1:0.1 hexane/ $CHCl_3$ /MeOH mixture as an eluent. The second green-colored fraction was collected (the first colored fraction was a trace of *t*-BuH<sub>2</sub>Pc). The solvent was evaporated, and further purification was achieved by gel-permeation chromatography on a Bio-Beads S-X1 column using  $CHCl_3$  as an eluent. After solvent evaporation, a dark-green residue was recrystallized twice from toluene with hexane to give **1b** as a green solid (yield: 0.01 g, 1.6%). Anal. (Calcd, Found for  $C_{50}H_{48}N_{12}O_2W_2$ ): C (49.36, 49.11), H (3.98, 4.52), N (13.81, 13.65). HR-MS ( $m/z$ ): [ $M^+$  + Na] calcd for  $C_{50}H_{48}N_{12}O_2W_2Na$ , 1239.2946; found, 1239.2934.  $^1H$  NMR (400 MHz,  $CDCl_3$ ):  $\delta$  10.04–9.73 (m, 8H), 8.60–8.56 (m, 4H), 1.88–1.86 (m, 36H). UV/vis/NIR ( $CCl_4$ )  $\lambda_{max}/nm$  ( $\epsilon/M^{-1} cm^{-1}$ ): 1405 (5000), 1073 (20000), 994 (42000), 913 (28000), 384 (48000).

**2.** A mixture of 5,6-di-4-*tert*-butylphenyl-1*H*-isindole-1,3(2*H*)-diimine (205 mg, 0.5 mmol),  $(NH_4)_2MoO_4$  (19.6 mg, 0.1 mmol), and urea (1.5 g, 25 mmol) was heated for 1 h from 160 to 220 °C. At 220 °C, 1-chloronaphthalene was added to the mixture, and the temperature was maintained for 30 min. After the reaction mixture was cooled to room temperature, **2** was extracted with  $CHCl_3$  and purified by column chromatography on silica gel (using first hexane and then  $CHCl_3$  as eluents, followed by toluene). The compound was recrystallized with MeOH to give **2** as a red powder (yield: 7.1 mg, 7.6%). HR-MS ( $m/z$ ): [ $M^+$ ] calcd for  $C_{114}H_{112}Mo_2N_{12}O_2$ , 1874.7176; found, 1874.7164.  $^1H$  NMR (400 MHz, toluene- $d_8$ ):  $\delta$  10.11 (s, 4H), 9.66 (s, 4H), 7.77–7.17 (br, 32H), 1.37–1.19 (s, 72H). UV/vis/NIR ( $CHCl_3$ )  $\lambda_{max}/nm$  ( $\epsilon/M^{-1} cm^{-1}$ ): 1190 (22000), 1045 (48000), 959 (94000), 461 (51000), 404 (85000).

**3.** A mixture of 4,5-di(4-*tert*-butylphenoxy)phthalonitrile (0.20 g, 0.50 mmol),  $(NH_4)_2MoO_4$  (0.050 g, 0.25 mmol), and urea (0.30 g, 5.0 mmol) was ground in an agate mortar. A small amount of 1-chloronaphthalene was added to the mixture, which was then heated at ca. 200 °C for 1 h under nitrogen. Urea (0.10 g, 1.8 mmol) was subsequently added, and the reactants were heated at ca. 220 °C. Urea (0.10 g, 1.8 mmol) was added three times after 3.5, 5.5, and 7 h. After the mixture was heated for ca. 10 h, the crude product was cooled to room temperature. Compound **3** was extracted with  $CHCl_3$  and purified by column chromatography on silica gel (using first hexane and then toluene as eluents). Further purification was achieved by gel-

permeation chromatography on a Bio-Beads S-X1 column using toluene as an eluent. After removal of the solvent under vacuum, the compound was obtained as a dark-red solid (yield: 0.81 mg, 0.32%). HR-MS ( $m/z$ ): [ $M^+$  + Na] calcd for  $C_{114}H_{112}Mo_2N_{12}O_{10}Na$ , 2026.6656; found, 2026.6625.  $^1H$  NMR (600 MHz,  $CDCl_3$ ):  $\delta$  9.37 (s, 4H), 9.23 (s, 4H), 7.58 (d,  $J$  = 8.8 Hz, 8H), 7.52 (d,  $J$  = 8.9 Hz, 8H), 7.33 (d,  $J$  = 8.8 Hz, 8H), 7.31 (d,  $J$  = 9.1 Hz, 8H), 1.51 (s, 36H), 1.42 (s, 36H).  $^{13}C$  NMR (150 MHz,  $CDCl_3$ ):  $\delta$  161.35, 155.36, 154.79, 153.57, 151.94, 149.61, 148.10, 146.74, 132.04, 131.97, 127.26, 126.93, 120.01, 117.76, 115.66, 112.99, 34.65, 34.49, 31.7, 31.6. UV/vis/NIR ( $CCl_4$ )  $\lambda_{max}/nm$  ( $\epsilon/M^{-1} cm^{-1}$ ): 1152 (11000), 1021 (23000), 937 (39000), 439 (23000), 402 (33000).

**4.** A stirred mixture of 4,5-di(phenylthio)phthalimide (0.73 g, 2.0 mmol), urea (1.21 g, 20.0 mmol), and ammonium molybdate (0.08 g, 0.4 mmol) was slowly heated for 45–50 min from 120 to 250 °C and then kept at that temperature for a further 10 min. After the reaction mixture was cooled and benzene was added, the crude product was collected by extraction and recrystallized three times from benzene solution by adding methanol. The dark-brown-colored material was purified by gel-permeation chromatography on a Bio-Beads S-X1 column (eluent  $CHCl_3$ ) and by recrystallization (twice) from  $CHCl_3$  solution with methanol, affording a wine colored solid (yield: 28.0 mg, 8.3%). Anal. (Calcd, Found for  $C_{82}H_{48}Mo_2N_{12}O_2S_8$ ): C (58.56, 57.67), H (2.88, 3.11), N (9.99, 9.65). Fast atom bombardment MS ( $m/z$ ): [ $M^+$ ] calcd for  $C_{82}H_{48}Mo_2N_{12}O_2S_8$ , 1681.7; found, 1682.  $^1H$  NMR (400 MHz,  $CDCl_3$ ):  $\delta$  7.78–7.39 (45H, SPh), 9.45, 9.41 (s, 8H). UV/vis/NIR ( $CCl_4$ )  $\lambda_{max}/nm$  ( $\epsilon/M^{-1} cm^{-1}$ ): 1180 (12000), 1057 (26000), 972 (34000), 471 (30000), 409 (33000), and 324 (41000). IR (KBr)  $cm^{-1}$ : 1580, 1541, 1508, 1474, 1439, 1417, 1341, 1300, 1250, 1152, 1100, 1065, 1020, 970, 856, 795, 748, 733, 704, 689, 638.

## ■ ASSOCIATED CONTENT

### ● Supporting Information

Mass data for all compounds; COSY spectra of **1a** and **3** in  $CDCl_3$ ; NOE spectrum of **3** in  $CDCl_3$ ;  $^{14}N$  NMR spectrum of compound **2**; ESR spectra of **1a**, **3**, and tetra-*tert*-butyl-substituted ( $Mo^V \equiv N$ )Pc in deaerated toluene at room temperature; geometry-optimized structure of substituent-free **2**; and complete ref 27. This material is available free of charge via the Internet at <http://pubs.acs.org>.

## ■ AUTHOR INFORMATION

### Corresponding Author

[rmeluk@niopik.ru](mailto:rmeluk@niopik.ru); [nagaok@m.tohoku.ac.jp](mailto:nagaok@m.tohoku.ac.jp)

### Notes

The authors declare no competing financial interest.

## ■ ACKNOWLEDGMENTS

This work was partly supported by the Moscow City Government, a Grant-in-Aid for Scientific Research on Innovative Areas (20108007, “pi-Space”) from the Ministry of Education, Culture, Sports, Science, and Technology (MEXT), and a Grant-in-Aid for Scientific Research (B) (23350095) from JSPS. O.M. thanks the Global Center of Excellence (G-COE) program of Tohoku University. A.M. is indebted to the JST PRESTO Program. The authors thank Prof. Takeaki Iwamoto and Dr. Shintaro Ishida (Tohoku University) for X-ray measurements, Prof. Seigo Yamauchi and Dr. Islam Saiful (Tohoku University) for EPR measurements, and Dr. Eunsang Kwon (Tohoku University) and JEOL RESONANCE Inc. for  $^{14}N$  NMR measurements.

## ■ REFERENCES

- (1) Linstead, R. P. *J. Chem. Soc.* **1934**, 1016–1017.

- (2) *Phthalocyanines: Properties and Applications*; Leznoff, C. C., Lever, A. B. P., Eds.; VCH: New York, 1989–1996; Vols. 1–4.
- (3) *The Porphyrin Handbook*; Kadish, K. M., Smith, K. M., Guillard, R., Eds.; Academic Press: New York, 2003; Vols. 15–20.
- (4) Torre, G.; Claessens, C. G.; Torres, T. *Chem. Commun.* **2007**, 2000–2015.
- (5) Jiang, J.; Kasuga, K.; Arnold, D. P. In *Supramolecular Photosensitive and Electroactive Materials*; Academic Press: New York, 2001.
- (6) Claessens, C. G.; Gonzalez-Rodriguez, D.; Torres, T. *Chem. Rev.* **2002**, *102*, 835–853.
- (7) Kobayashi, N. In *The Porphyrin Handbook*; Kadish, K. M., Smith, K. M., Guillard, R., Eds.; Academic Press: New York, 2003; Vol. 15, Chapter 100.
- (8) Engel, M. K. In *The Porphyrin Handbook*; Kadish, K. M., Smith, K. M., Guillard, R., Eds.; Academic Press: New York, 2003; Vol. 20, Chapter 122.
- (9) (a) Moser, F. H.; Thomas, A. L. *The Phthalocyanines*, CRC Press: Boca Raton, FL, 1983; Vols. I and II. (b) In *Phthalocyanines: Properties and Applications*; Leznoff, C. C., Lever, A. B. P., Eds.; VCH: New York, 1989; Vol. 1, Chapter 1. (c) McKeown, N. B. In *The Porphyrin Handbook*; Kadish, K. M., Smith, K. M., Guillard, R., Eds.; Academic Press: New York, 2003; Vol. 15, Chapter 18. (d) Nemykin, V. N.; Luk'yanets, E. A. In *Handbook of Porphyrin Science*; Kadish, K. M., Smith, K. M., Guillard, R., Eds.; World Scientific: Singapore, 2010; Vol. 3, Chapter 11. (e) Luk'yanets, E. A.; Nemykin, V. N. *J. Porphyrins Phthalocyanines* **2010**, *14*, 1–40.
- (10) Crystallographic data for **2**:  $C_{124}H_{119}N_{12}O_2Mo_2Cl$ , MW = 2036.64, monoclinic, space group  $C2/c$  (No. 15),  $a = 52.893(12)$  Å,  $b = 14.406(3)$  Å,  $c = 39.178(7)$  Å,  $\beta = 104.803(4)^\circ$ ,  $V = 28863(10)$  Å<sup>3</sup>,  $Z = 8$ ,  $\rho_{\text{calc'd}} = 0.937$  g/cm<sup>3</sup>,  $T = -173$  °C, 66048 measured reflns, 25359 unique reflns ( $R_{\text{int}} = 0.0820$ ),  $R = 0.0657$ ,  $R_w = 0.1853$  (all data), GOF = 0.889.
- (11) According to geometry optimization calculations for the substituent-free **2** structure, *cis-2* is predicted to be more stable than *trans-2* by 13.1 kcal/mol, although the  $\pi$  systems of *cis-2* and *trans-2* are both predicted to adopt domed structures (the energy difference was based on the total energies corrected with the zero-point vibrational energies). This may provide an explanation for why we obtained only the *cis-2* structure as an isolable product.
- (12) Modéc, B.; Sala, M.; Clerac, R. *Eur. J. Inorg. Chem.* **2010**, 542–553.
- (13) (a) Matz, K. G.; Mtei, R. P.; Leung, B.; Burgmayer, S. J. N.; Kirk, M. L. *J. Am. Chem. Soc.* **2010**, *132*, 7830–7831. (b) Groyzman, S.; Wang, J.-J.; Tagore, R.; Lee, S. C.; Holm, R. H. *J. Am. Chem. Soc.* **2008**, *130*, 12794–12807. (c) Wang, J.-J.; Holm, R. H. *Inorg. Chem.* **2007**, *46*, 11156–11164. (d) Basu, P.; Nemykin, V. N.; Sengar, R. S. *Inorg. Chem.* **2009**, *48*, 6303–6313. (e) Carrano, C. J.; Chohan, B. S.; Hammes, B. S.; Kail, B. W.; Nemykin, V. N.; Basu, P. *Inorg. Chem.* **2003**, *42*, 5999–6007. (f) Inscore, F. E.; Knottenbelt, S. Z.; Rubie, N. D.; Joshi, H. K.; Kirk, M. L.; Enemark, J. H. *Inorg. Chem.* **2006**, *45*, 967–976. (g) Mader, M. L.; Carducci, M. D.; Enemark, J. H. *Inorg. Chem.* **2000**, *39*, 525–531.
- (14) Mizutani, J.; Imoto, H.; Saito, H. *Acta Crystallogr.* **1997**, *C53*, 47–50.
- (15) Maree, S.; Nyokong, T. *J. Porphyrins Phthalocyanines* **2001**, *5*, 782–792.
- (16) Gorsch, M.; Kienast, A.; Huckstadt, H.; Homborg, V. Z. *Anorg. Allg. Chem.* **1997**, *623*, 1433–1440.
- (17) Frick, K.; Verma, S.; Sundermeyer, J. *Eur. J. Inorg. Chem.* **2000**, 1025–1030.
- (18) (a) Kobayashi, N.; Nakajima, S.; Ogata, H.; Fukuda, T. *Chem.—Eur. J.* **2004**, *10*, 6294–6312. (b) Kobayashi, N.; Fukuda, T. *Chem. Lett.* **2004**, *33*, 32–33. (c) Fukuda, T.; Makarova, E. A.; Luk'yanets, E. A.; Kobayashi, N. *Chem.—Eur. J.* **2004**, *10*, 117–133. (d) Makarova, E. A.; Fukuda, T.; Luk'yanets, E. A.; Kobayashi, N. *Chem.—Eur. J.* **2005**, *11*, 1235–1250.
- (19) (a) Nyokong, T. *Inorg. Chim. Acta* **1989**, *160*, 235–239. (b) Nyokong, T. *Polyhedron* **1994**, *13*, 215–220.
- (20) A <sup>14</sup>N NMR spectrum was recorded for **2** (Figure S5 in the SI). The signal was measured between –1000 and 800 ppm, but only a single peak was observed at –66 ppm. If the structure of **2** were consistent with that of **5B** in its core structure, at least two <sup>14</sup>N NMR peaks would be anticipated. Although the <sup>1</sup>H NMR data can be interpreted for both structures **5A** and **5B** (Figure 3), this result also supports the characterization of **2** as **5A**.
- (21) Gouterman, M. In *The Porphyrins*; Dolphin, D., Ed.; Academic Press: New York, 1978; Vol III, Part A, Chapter 1.
- (22) Platt, J. R. *J. Chem. Phys.* **1949**, *17*, 484–495.
- (23) Mack, J.; Stillman, M. J. In *The Porphyrin Handbook*; Kadish, K. M., Smith, K. M., Guillard, R., Eds.; Academic Press: New York, 2003; Vol. 16, Chapter 103.
- (24) Mack, J.; Stillman, M. J.; Kobayashi, N. *Cood. Chem. Rev.* **2007**, *251*, 429–453.
- (25) Kobayashi, N.; Nakai, K. *Chem. Commun.* **2007**, 4077–4092.
- (26) (a) Mack, J.; Asano, Y.; Kobayashi, N.; Stillman, M. J. *J. Am. Chem. Soc.* **2005**, *127*, 17697–17711. (b) Kobayashi, N.; Miwa, H.; Nemykin, V. N. *J. Am. Chem. Soc.* **2002**, *124*, 8007–8020. (c) Kobayashi, N.; Fukuda, T. *J. Am. Chem. Soc.* **2002**, *124*, 8021–8034. (d) Asano, Y.; Muranaka, A.; Fukasawa, A.; Hatano, T.; Uchiyama, M.; Kobayashi, N. *J. Am. Chem. Soc.* **2007**, *129*, 4516–4517. (e) Fukuda, T.; Masuda, S.; Kobayashi, N. *J. Am. Chem. Soc.* **2007**, *129*, 5472–5479. (f) Takeuchi, Y.; Matsuda, A.; Kobayashi, N. *J. Am. Chem. Soc.* **2007**, *129*, 8271–8281. (g) Mack, J.; Bunya, M.; Shimizu, Y.; Uoyama, H.; Komobuchi, N.; Okujima, T.; Uno, H.; Ito, S.; Stillman, M. J.; Ono, N.; Kobayashi, N. *Chem.—Eur. J.* **2008**, *14*, 5001–5020. (h) Kuzuhara, D.; Mack, J.; Yamada, H.; Okujima, T.; Ono, N.; Kobayashi, N. *Chem.—Eur. J.* **2009**, *15*, 10060–10069. (i) Kobayashi, N.; Narita, F.; Ishii, K.; Muranaka, A. *Chem.—Eur. J.* **2009**, *15*, 10173–10181. (j) Shimizu, S.; Zhu, H.; Kobayashi, N. *Chem.—Eur. J.* **2010**, *16*, 11151–11159. (k) Okujima, T.; Jin, G.; Matsumoto, N.; Mack, J.; Mori, S.; Ohara, K.; Ando, C.; Ono, N.; Yamada, H.; Uno, H.; Kobayashi, N. *Angew. Chem., Int. Ed.* **2011**, *50*, 5699–5703. (l) Mack, J.; Kobayashi, N. *Chem. Rev.* **2011**, *111*, 281–321.
- (27) Frisch, M. J.; et al. *Gaussian 03*, revision E.01; Gaussian, Inc.: Wallingford, CT, 2004.
- (28) Muranaka, A.; Matsushita, O.; Yoshida, K.; Mori, S.; Suzuki, M.; Furuyama, T.; Uchiyama, M.; Osuka, A.; Kobayashi, N. *Chem.—Eur. J.* **2009**, *15*, 3744–3751.
- (29) Michl, J. *J. Am. Chem. Soc.* **1978**, *100*, 6801–6811.
- (30) Michl, J. *Pure Appl. Chem.* **1980**, *52*, 1549–1563.
- (31) Chen, Z. F.; Wannere, C. S.; Corminboeuf, C.; Puchta, R.; Schleyer, P. v. R. *Chem. Rev.* **2005**, *105*, 3842–3888.
- (32) Kamino, S.; Horio, Y.; Komeda, S.; Minoura, K.; Ichikawa, H.; Horigome, J.; Tatsumi, A.; Kaji, S.; Yamaguchi, T.; Usami, Y.; Hirota, S.; Enomoto, S.; Fujita, Y. *Chem. Commun.* **2010**, *46*, 9013–9015. In particular, see Figure S10.
- (33) Sheldrick, G. M. *SHELXL-97: Program for the Solution and Refinement of Crystal Structures*; University of Göttingen: Göttingen, Germany, 1997.
- (34) Mikhaleiko, S. A.; Barkanova, S. V.; Lebedev, O. L.; Luk'yanets, E. A. *J. Gen. Chem. USSR (Engl. Transl.)* **1971**, *41*, 2770–2773.
- (35) Solov'yova, L. I.; Luk'yanets, E. A. *Coll. "Anilino-krasochennaya Promyshlennost", Niitekhnim. (Russ.)* **1976**, *9*, 1.
- (36) Piechocki, C.; Simon, J. *Nouv. J. Chim.* **1985**, *9*, 159–166.